

SNN-SC: A Spiking Semantic Communication Framework for Feature Transmission

Mengyang Wang, Jiahui Li, *Member, IEEE*, Mengyao Ma, *Member, IEEE*,
Xiaopeng Fan, *Senior Member, IEEE*, Yonghong Tian, *Fellow, IEEE*,

Abstract—In Collaborative Intelligence (CI), Artificial Intelligence (AI) models are split between edge devices and cloud. Features extracted from input on edge devices are transmitted to the cloud for subsequent tasks. Extracting task-related and compact information is critical when transmission bandwidth is limited. In this paper, we propose a task-oriented Semantic Communication (SC) framework (SNN-SC) to address this problem. In SC, only important information for downstream tasks is extracted and transmitted. However, most of the existing SC works only transmit analog information on the AWGN channel and cannot be directly used for digital channels. SNN-SC fills this gap by using Spiking Neural Networks (SNNs) to extract and transmit semantic information. Since the outputs of SNNs are binary spikes, SNN-SC can be directly applied to digital channels. In SNN-SC, a new spiking neuron is proposed to help the cloud recover binary semantic information into informative floating-point features. Furthermore, we improve the performance of SNN-SC by maximizing the entropy of the semantic information. We evaluate the performance of SNN-SC on different collaborative classification models, digital channels, and bandwidths. The experimental results show that SNN-SC is more robust than the CNN-based SC framework and separate source and channel coding method on digital channels.

Index Terms—Collaborative intelligence, semantic communication, digital communication, spiking neural network.

I. INTRODUCTION

THE problem Collaborative Intelligence (CI) tries to solve is that the deep model is too complex and computationally expensive to run on mobile devices [1]. Therefore, the model is divided into two parts: the edge device part and the cloud part, and these two parts complete the computation of the whole model collaboratively [2], [3]. The edge device obtains input information such as images and videos and uses the part of the deep model to extract features. Then the features are sent to the edge server for subsequent task execution [4],

This work was supported in part by the National Key R&D Program of China (2021YFF0900500), the National Natural Science Foundation of China (NSFC) under grants U22B2035 and 62272128. (*Corresponding author: Xiaopeng Fan.*)

Mengyang Wang and Xiaopeng Fan are with the School of Computer Science, Harbin Institute of Technology, Harbin 150001, China, and also with Peng Cheng Laboratory, Shenzhen 519055, China (e-mail: mywang1996@outlook.com; fxp@hit.edu.cn).

Jiahui Li and Mengyao Ma are with the Wireless Technology Lab, Huawei, Shenzhen 518129, China (e-mail: lijiahui666@huawei.com; ma.mengyao@huawei.com).

Yonghong Tian is with the School of Electrical Engineering and Computer Science, Peking University, Beijing, China, 100871, and also with Pengcheng Laboratory, No. 2, Xingke 1st Street, Nanshan, Shenzhen, China 518000 (e-mail: yhtian@pku.edu.cn).

[5]. Since the transmission of raw features may require a large amount of channel bandwidth, it is critical to encode the data into an informative and compact representation for low-latency inference. In this paper, we use the theory of semantic communication to design a model to solve this problem.

According to *A mathematical theory of communication* [6], semantic-level communication (i.e., semantic communication, SC) only transmits useful, essential, and relevant information of the source, further reducing bandwidth consumption while maintaining task performance [7]. However, quantifying semantic information is challenging due to the lack of precise mathematical models. The breakthroughs of deep learning (DL) [8] make it possible to tackle many challenges without requiring a mathematical model.

Recently, Artificial Neural Networks (ANNs) such as Convolutional Neural Networks (CNNs), Fully Connected Neural Networks (FCNNs), and Recurrent Neural Networks (RNNs) have shown great potentials to design end-to-end communication systems [9], [10]. Naturally, DL-based SC frameworks are also proposed, which use ANNs based semantic encoder and semantic decoder to transmit necessary information relevant to the specific task at the receiver. To improve transmission robustness, especially when communication resources are limited and noise power is high, most SC systems adopt Joint Source-Channel Coding (JSCC) [11] [12]. At present, DL-based SC studies are mainly applied in text [11], [13], [14], image [15]–[18] and deep feature [19]–[22] transmission. The SC framework for feature transmission can be an effective tool in CI [23], which reduces feature transmission overhead while maintaining task performance in the cloud.

However, since the outputs of ANNs are floating-point numbers, most DL-based SC frameworks [15]–[22], [24]–[28], [11], [13], [14] are only trained and tested on the additive white Gaussian noise (AWGN) channel or other analog channels to transmit extracted semantic information. Although the digital channels are considered in [20] and [21], they add additional quantization steps to binarize the information before transmission which adds additional computational overhead. In practical scenarios, digital communication systems that transmit bitstreams are more widely used. Therefore, we aim to design an end-to-end SC framework for feature transmission under digital channels such as Binary Symmetric Channel (BSC) and Binary Erased Channel (BEC), without explicit quantization.

Today, Spiking Neural Networks (SNNs) are seen as the third generation of neural network models [29], which operate similarly to biological neurons in the brain [30]. The exchange

information between spiking neurons are discrete action potentials (spikes) represented by 0s and 1s, making the energy consumption of SNN lower than ANN [31]. More importantly, SNNs can exploit temporal information by iteratively running multiple time steps [32]. The spiking neuron accumulates the input as its membrane potential at each time step, and when the membrane potential exceeds a threshold, the neuron will fire a spike to the connected neuron and reset the membrane potential [33], [34]. Currently, SNNs are widely used for AI tasks, and by running multiple time steps, SNNs can get very close performance to ANN models [35]–[39]. Since the output of a spiking neuron is a binary spike, we can think of it as a binary encoder without explicit quantization.

Based on the idea of SC and the characteristics of SNN, in this paper, we propose an SNN-based SC framework: SNN-SC, which solves the problem of efficiently performing edge-cloud inference on digital channels for models in CI scenarios. The SNN-SC is trained in a task-oriented manner, i.e., targeting the downstream inference task rather than feature reconstruction. In order to evaluate the feasibility of SNN-SC, we use SNN-SC to transmit features of different edge-cloud collaborative classification models under different channels and bandwidths. The two baseline methods are a CNN-based SC model with a similar structure to SNN-SC but uses a quantization step to binarize features, and a traditional communication scheme uses source coding and channel coding separately. To the best of our knowledge, this is the first work to build a digital feature SC model for CI, which extracts semantic information via SNNs for task-oriented digital communication. The main contributions of this paper are summarized as follows:

- 1) We propose an SNN based SC framework for CI under digital communication, named SNN-SC, where transceiver is jointly designed to perform digital semantic communication via SNN. Based on the nature of the binary output of spiking neurons, SNN-SC can operate directly on digital channels without explicit quantization.
- 2) We propose a novel spiking neuron Integrate and Hybrid Fire (IHF) that outputs both spike and membrane potential information, to help the cloud recover the binary semantic information into informative floating-point features.
- 3) We find that maximizing the entropy of semantic information transmitted on digital channels can improve the efficiency of SNN-SC in transmitting semantic information, thereby improving the performance of cloud tasks.
- 4) The image classification task is adopted as an example to demonstrate the effectiveness of SNN-SC. Experimental results show that the SNN-SC model is more robust than the CNN-based SC framework and separate source and channel coding method on digital channels.

The rest of this paper is organized as follows. Section II reviews some related works. Section III describes the architecture, spiking neurons and training method of the proposed SNN-SC. Experiments and ablation analysis are presented in Section IV to verify the effectiveness of our methods. Section V finally concludes this paper.

II. RELATED WORKS

A. ANN-Based Semantic Communication

The great success of DL enables SC systems to work well in limited bandwidth and noisy channels. Existing works on ANN-based SC are mainly applied in three scenarios: text transmission, image transmission, and feature transmission.

In text transmission, SC focuses on recovering the meaning of sentences. [13] proposes an SC system DeepSC for transmitting sentences, in addition to the Transformer-based semantic encoder and decoder in the model, AWGN channel is also interpreted as a layer. They also design a new measure named sentence similarity based on BERT [40] to accurately reflect the performance of the DeepSC at the semantic level. To make the DeepSC affordable for Internet-of-Things (IoT) devices, [14] proposes a lite distributed version of DeepSC called L-DeepSC, which reduces model complexity by pruning model redundancy and reducing weight resolution. Furthermore, [11] and [41] introduces hybrid automatic repeat request (HARQ) to reduce the semantic error caused by the channel interference, for sentences with varying lengths. To help the receiver recover the text, [42] proposes a context-based dynamic programming algorithm for decoder, [43] proposes an iterative decoder, where the intermediate decoded text is then used as a prior information for the decoder in the next iteration.

In image transmission, SC focuses on reconstructing the pixels of the image. In [15], an end-to-end SC framework for transmitting images is built by a multi-layer Auto-Encoder (AE) [44], and the AWGN channel and Rayleigh slow fading channel are also modeled as the non-trainable layer, introducing random corruption to the transmitted semantic information. By jointly optimizing the encoder and decoder under the noisy channel, the input image can be robustly transmitted on the AWGN channel. The measurement in image transmission is the peak signal-to-noise ratio (PSNR), which describes the difference between the pixels of the reconstructed image and the original image. With the deepening of research, [16] and [17] propose SC models to adapt channels with different signal-to-noise ratios (SNRs). [16] proposes a new training strategy, which trains the model under channels with randomly varying SNRs. [17] proposes a new attention module that uses SNR information to enhance the robustness of semantic encoding. Considering the distributed scenario, [18] designs an SC framework with two encoders, which transmits a pair of correlated images over independent channels and jointly recovers them by one decoder.

In feature transmission, SC focuses on task performance, which is affected by the reconstructed feature at the receiver. [19] and [20] design AE-based feature SC models to transmit semantic information of the intermediate features in the image retrieval model and the classification model, respectively. The measurement in feature transmission is downstream task performance, such as classification accuracy, etc. [21] and [22] design SC models for the features of the multi-task model and the multi-modal model transmitted through AWGN channel. [26] leverages an information bottleneck (IB) framework to formalize a rate-distortion trade-off between

the informativeness of the encoded semantic information and the inference performance. To reduce the computational cost, [25] uses filter pruning strategy on the classification model and [27] adds branch networks on the point-cloud processing model for early exiting in CI scenario. [28] and [45] study collaborative semantic communication, where the features of correlated source data among different users are transmitted via a shared channel, then fused at the cloud to perform retrieval or identification task.

As we can see, the ANN enabled SC works are applied on various kinds of data, and the feature SC framework is the effective tool in CI. Moreover, since the output of the neural network is all floating-point numbers, most SC works only do experiments on the analog channel like AWGN or Rayleigh slow fading channel, and only [11] and [20] consider the digital channel. However, in [11] and [20], the quantization steps required to binarize information is not only non-differentiable but also adds computational overhead. In this paper, we investigate the feature SC framework for CI under digital channels, which does not require explicit quantization and can be directly applied to digital channels.

B. Spiking Neural Networks

Unlike traditional deep learning models that convey information using continuous decimal values, SNNs use binary spikes to transmit information. Spiking neurons are the basic computational unit of SNNs, and they receive continuous values input and convert them into spikes. Most spiking neurons operate in three main steps: charge, fire, and reset [32]. At each time step, these three steps are executed in sequence. We take Integrate-Fire (IF) [46] neuron as an example to introduce its working process.

When charging, IF receives the weighted input from previous layer at current time step as the membrane potential, and the iterative model of charging can be modeled as

$$m_i^t = m_i^{t-1} + I_{i-1}^t, \quad (1)$$

where m_i^t represents the membrane potential of i^{th} neuron, and I_{i-1}^t is the weighted input from previous layer at time step t .

After charging, the fire step can be modeled as

$$S_i^t = \begin{cases} 1, & m_i^t > V_{th}, \\ 0, & \text{otherwise,} \end{cases} \quad (2)$$

where S_i^t of Eq. (2) is the output spike of neuron i at time step t , and V_{th} is the firing threshold of the neuron. When the membrane potential exceeds the threshold, the neuron will output a spike at the current time step.

After firing a spike, the membrane potential will be reset, and it can be modeled as

$$m_i^t = \begin{cases} (1 - S_i^t)m_i^t + S_i^t V_{reset} & (\text{hard reset}), \\ m_i^t - S_i^t V_{th} & (\text{soft reset}), \end{cases} \quad (3)$$

there are two reset methods as shown in Eq. (3): hard reset and soft reset. In hard reset, the membrane potential is directly set to the preset value V_{reset} [47]. On the other hand, the membrane potential is subtracted by the threshold V_{th} in soft

reset [48]. What's more, if the membrane potential is less than the threshold, a '0' spike occurs and the membrane potential does not change after the reset step.

In addition to the IF that outputs binary spikes, there are spiking neurons like membrane potential (MP) neuron [49] that outputs membrane potential values after the charge step.

Since the fire step is non-differentiable, the training methods of SNNs are proposed. Nowadays, the ANN-to-SNN conversion [35], [37], [50], [51] and backpropagation with surrogate gradient are the two main methods [30], [49], [52], [53]. The ANN-to-SNN method first trains a neural network using rectified linear unit (ReLU) as the activation function, then replaces the ReLU with spiking neurons. However, the performance of SNNs resulting from direct conversion is generally poor. Therefore, additional operations such as normalization [54], [55] or threshold adjustment [34], [36] are required. The backpropagation method constitutes a continuous relaxation of the non-smooth firing to enable backpropagation with a surrogate gradient. With this approach, SNNs can be trained end-to-end and achieve competitive performance with ANNs.

C. SNN-Based Semantic Communication

With the development of SNNs, some works has been carried out to build SC systems for spikes via SNNs.

[56] proposes NeuroJSCC, an end-to-end SC system for the spike data. NeuroJSCC first uses an SNN to extract information from the input spike train, and then the output spikes are modulated into analog signals by Impulse Radio (IR) [57] and transmitted to the receiver through a Gaussian channel. The receiver first quantizes the signals into binary spikes, which are then decoded to perform the classification task. [58] is an extended version of [56]. [58] considers a distributed SC, where multiple devices transmits their semantic information to an edger sever through a shared multi-path fading channel.

Based on these related works, we find that the SNN-based SC for digital communication is blank. In this paper, we use SNN to build an SC model, SNN-SC, which transmits the semantic information of the features of the model in CI scenario. Since spiking neurons can convert continuous inputs into binary spikes without explicit quantization, SNN-SC can be directly applied to digital communication.

III. METHODOLOGY

A. Overview of the SNN-SC

We consider the feature SC in CI under digital channel. In Fig. 1, a image classification model is segmented and deployed on edge device and cloud, the part in the edge device is called the feature extraction part, and the part in the cloud is called the task execution part. The proposed SNN-SC extracts binary semantic information from features via SNN at the edge device side, and then directly transmits them through digital channels. In the cloud, SNN-SC uses SNN to restore the received semantic information and convert it into floating point features to ensure the operation of the subsequent task execution module. Furthermore, as can be seen see from Fig. 1 that SNN-SC framework consists of two parts, the encoder

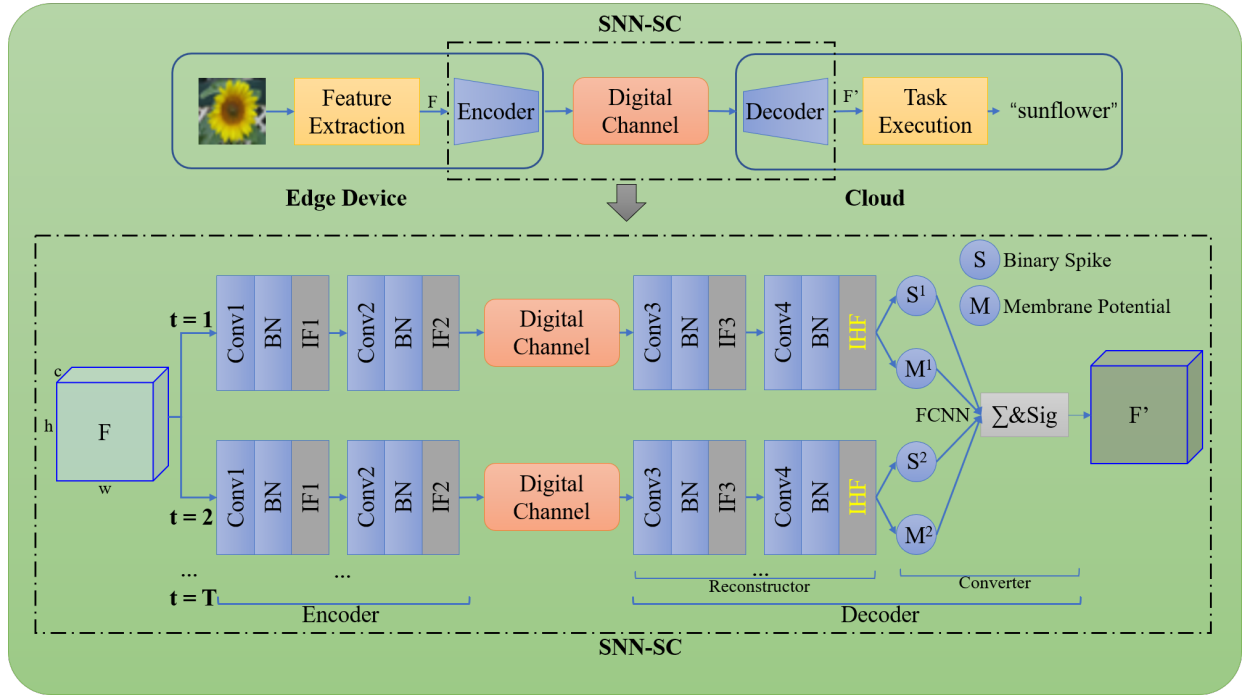


Fig. 1. The architecture of the SNN-SC model over digital channel.

and the decoder, where the decoder consists of a reconstructor and a converter.

The input of SNN-SC is the output feature of the feature extraction part. At each time step, we directly feed the floating-point feature into SNN-SC, the SNN-based encoder extracts compact semantic information and converts it into spikes, and the extracted semantic information is transmitted to the reconstructor through a digital channel. The SNN-based reconstructor receives the semantic information and outputs two results: a binary feature \mathbf{S} composed of spikes and an analog feature \mathbf{M} composed of current membrane potential.

After the encoder and reconstructor run T time steps, all outputs of the reconstructor are fused by an FCNN-based converter to obtain the final reconstructed feature.

During the iterative running of SNN-SC, the model parameters in the encoder and reconstructor are shared across all time steps, except for the spiking neurons. Spiking neurons charge, fire, and reset at each time step, so that the membrane potential has different states at different time steps.

B. Details of the SNN-SC

The structures of the encoder and reconstructor are inspired by the CNN-based SC frameworks, which are multi-layer AEs. In this paper, a multi-layer SNN-based AE is constructed as an SC framework of intermediate features to enable semantic communication over digital channels.

In the encoder, there are two *Conv-BN-IF* modules, where *Conv* is the convolutional layer, *BN* is the batch normalization layer, and *IF* is the integrate-fire neuron as the activation function [46]. Since the input of the encoder is a feature with float-points values, the first *Conv-BN-IF* is used to encode the float values into spikes (e.g. direct encoding [54],

[59]), preliminarily compress the feature and extract semantic information. Then the second *Conv-BN-IF* further compresses the spiking feature and extracts semantic information. Suppose the dimension of the input feature is (c, h, w) , corresponding to (channel, height, width), and the output feature dimensions of the first module and the second module are (c_1, h_1, w_1) and (c_2, h_2, w_2) , respectively. To extract compact semantic information, the size relationship among these dimensions is as follows: $c * h * w > c_1 * h_1 * w_1 > c_2 * h_2 * w_2$. For the deep feature $F \in \mathbb{R}^{c \times h \times w}$ comes from the feature extraction model on the edge device, the semantic extracting process at time step t can be expressed as:

$$z^t = E_{\theta_2}^2(E_{\theta_1}^1(F)), \quad (4)$$

where $E_{\theta_1}^1$ and $E_{\theta_2}^2$ indicate the first and second *Conv-BN-IF* modules with parameters as θ_1 and θ_2 , respectively. $z^t \in \{0, 1\}^{c_2 \times h_2 \times w_2}$ ($t \in \{1, \dots, T\}$) is the compact semantic information at the current time step t , consisting of binary spikes.

Then the extracted semantic information is directly transmitted to the reconstructor through digital channels such as BSC or BEC, with a bit error/erase rate p . In BSC, bits are flipped randomly with a certain probability (i.e. bit error rate). In BEC, bits are erased randomly with a certain probability (i.e. bit erase rate), and the erased bits are set to 0 or 1 with equal probability at the receiver. The transmission process from the encoder to the reconstructor can be expressed as:

$$\hat{z}^t = \eta(z^t, p), \quad (5)$$

where η represents the digital channel model, p represents the error probability of each bit in the bitstream, and \hat{z}^t is the interfered version of z^t . Since z^t is binary semantic

information, the amount of data transmitted on the channel at each time step is $c_2 * h_2 * w_2$ bits.

The reconstructor receives and decodes the interfered semantic information. Similar to the encoder, there are also two modules in the reconstructor. The first module *Conv-BN-IF* preliminarily decompresses the received semantic information, and the output feature dimension is (c_1, h_1, w_1) . Then the second module *Conv-BN-IHF* further decompresses the spiking feature and outputs two features: the feature $S^t \in \{0, 1\}^{c \times h \times w}$ composed of spikes and the feature $M^t \in \mathbb{R}^{c \times h \times w}$ composed of current membrane potential of **IHF**. Although these two features have different values, they have the same dimension as the original feature F , that is, (c, h, w) . The reconstructing process can be expressed as:

$$S^t, M^t = \mathbf{R}_{\phi_2}^2(\mathbf{R}_{\phi_1}^1(z^t)), \quad (6)$$

where $\mathbf{R}_{\phi_1}^1$ and $\mathbf{R}_{\phi_2}^2$ indicate the modules *Conv-BN-IF* and *Conv-BN-IHF* with parameters as ϕ_1 and ϕ_2 , respectively. It should be noted that the **IHF** neuron is a new spiking neuron proposed in this paper, which can output two kinds of information, and we will introduce it in detail in the next section.

After the encoder and reconstructor run \mathbf{T} time steps, there are a total $2\mathbf{T}$ output features. To obtain the final reconstructed features, an FCNN-based converter is used to weighted and summed all output features of the reconstructor, and Sigmoid is the activation function. The converting process can be expressed as:

$$F' = \mathbf{C}_\psi([S^1, M^1, \dots, S^T, M^T]), \quad (7)$$

where \mathbf{C}_ψ indicate the converter with parameters as ψ , $F' \in \mathbb{R}^{c \times h \times w}$ is the final reconstructed feature with float-points values at receiver, which has the same dimension as original feature F , and it will be input into the task execution network to perform subsequent image classification.

C. Integrate and Hybrid Fire neuron (IHF)

Based on our observations, we found that both IF, which outputs binary spikes, and MP [49], which outputs membrane potential values, output limited information. Therefore, we hope to combine the working principles of these two neurons to enrich the output information of spiking neurons.

To fully utilize the information of spiking neurons, we propose an IHF neuron that outputs both spike and membrane potential values. Unlike existing SNN neurons, IHF has four working steps. The first three working steps of IHF neuron are the same as IF neuron, and then IHF adds another output step after the reset step. The added step outputs the current membrane potential value, so the IHF neuron can be viewed as a combination of IF neuron and MP neuron.

However, the step of IHF outputting membrane potential is not exactly the same as that of MP outputting membrane potential. IHF outputs the membrane potential after the reset step, while MP outputs the membrane potential after the charge

step. The working process of the IHF neuron with soft reset in $\mathbf{R}_{\phi_2}^2$ in Eq. (6) can be modeled as:

$$m_i^t = m_i^{t-1} + I_{i-1}^t, \quad (8a)$$

$$S_i^t = \begin{cases} 1, & m_i^t > V_{th}, \\ 0, & \text{otherwise}, \end{cases} \quad (8b)$$

$$m_i^t = m_i^t - S_i^t V_{th}, \quad (8c)$$

$$M_i^t = m_i^t, \quad (8d)$$

where m_i^t, I_{i-1}^t are the membrane potential value and input from the previous layer at time step t , and V_{th} is the firing threshold of the IHF neuron. In particular, S_i^t, M_i^t are the binary and analog outputs of the IHF neuron at the time step t . Eq. (8a), Eq. (8b), Eq. (8c) and Eq. (8d) represent the charge, fire spike, soft reset and fire analog membrane potential steps of IHF, respectively. The change of IHF membrane potential with soft reset over time step is shown in Fig. 2. We can find that the IHF outputs the current membrane potential value (i.e., Output MP) at each time step. If the membrane potential exceeds the firing threshold, IHF will output a spike, and then the membrane potential will be reset before output.

In brief, IHF outputs two kinds of information at each time step. As IHF neurons output more information than IF and MP, making subsequent converter work well.

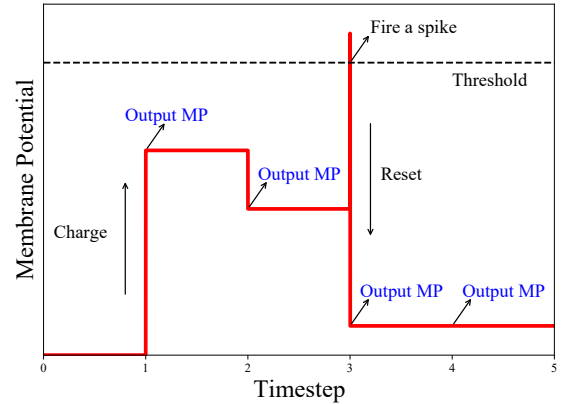


Fig. 2. The change of IHF membrane potential.

D. Training Strategy

In this paper, SNN-SC is used to transmit the semantic information from features in edge-cloud image classification model. For ease of understanding, ResNet50 (Residual Network) [60] is adopted as an example, and the training strategy of the whole framework is a stepwise strategy.

Since directly training the classification network combined with SNN-SC from scratch shows slow convergence [20], we propose a three-step training strategy to comprehensively train the entire model. Similar training strategies can also be used when the SNN-SC is applied to other classification networks.

The first step is to train ResNet50 end-to-end using the cross-entropy (CE) loss function. After ResNet50 converges, we choose an intermediate feature as the split point to divide

ResNet50 into the edge device part and the cloud part. SNN-SC is put at the split point to extract and transmit semantic information through digital channels like Fig. 1, and SNN-SC will run iteratively for T time steps.

The second step is to train the SNN-SC framework while keeping the parameters of the ResNet50 fixed. The loss function is defined in terms of the cloud classification task loss CE and the average entropy of the bits transmitted through the digital channel, which can be modeled as

$$\mathcal{L}_{total} = \mathcal{L}_{CE} + (\alpha - H)^2, \quad (9)$$

where \mathcal{L}_{CE} is the classification task loss CE, and H is the average entropy of the transmitted semantic information. We argue that entropy can be used to measure the amount of task-relevant information contained in the extracted semantic information. Since digital channels will cause the loss of semantic information, maximizing the entropy of the extracted semantic information is beneficial to improve the performance of cloud tasks. Given $z^t \in \{0, 1\}^{c \times h \times w}$ as the extracted semantic information at time step t , according to the Shannon entropy in [6], the average entropy of z^t can be calculated by

$$H = -(p_0 \log_2 p_0 + p_1 \log_2 p_1), \quad (10)$$

where p_0 and p_1 represents the probability that the bit is 0 and 1, respectively. We estimate p_0 and p_1 by the frequency of 0 and 1 in z^t . In Eq. (9), we constrain the entropy of semantic information by adding a regularization term to the original CE loss function. The parameter α is set to 1.0 according to the experiment, which maximizes the entropy of the semantic information. Since SNN-SC can be trained end-to-end by using the surrogate gradient, the entropy of semantic information will gradually approach the value of α during training. In this paper, we use the Sigmoid function as a surrogate function for the firing step when gradient backpropagation.

The third step is to jointly fine-tune the whole model. The whole model is trained end-to-end, and the loss function of this step is the same as the second step, but with a lower learning rate.

As mentioned earlier, SNN-SC is a task-oriented SC framework, so we only care about the classification task in the cloud, not whether the decoder perfectly reconstructs the original features. In this case, the loss function does not consider the symbol-level distance between the original features and the reconstructed features, and the classification accuracy of the model in the cloud is the evaluation metric of SNN-SC.

IV. EXPERIMENTS AND RESULTS

A. Experiment Setup

In this paper, the entire model is trained and evaluated on the CIFAR-100 [61] image classification dataset. In CIFAR-100, there are 60,000 32×32 color images, which are divided into 100 categories, and each category has 600 images. Since the edge devices usually collect and deal with low-resolution images in IoT devices, CIFAR-100 is well suited for on-device applications. The classification model used for CI is ResNet50 (Residual Network) [60] and VGG16 (Visual Geometry Group) network [62].

In addition, we use Pytorch [63] to build the model, and SNN-SC is built by SpikingJelly [64], which is an open-source deep learning framework for SNN based on PyTorch. Training and inference processes are performed on Tesla V100 GPUs.

B. Baseline Methods

We consider two cases for the baseline methods: the CNN-based SC framework, and the typical separate source and channel coding.

1) *CNN-based SC framework*: The CNN-based SC framework is an improved version of BottleNet++ [20]. To eliminate the impact of the network structure on performance, this framework uses the same network structure as SNN-SC, except for the activation function. In order to fit this model into the digital channel, the quantization step is added at the end of the encoder. Since the output is constrained by the Sigmoid function in $[0, 1]$, the quantization process is $X^q = \text{round}(X * (2^n - 1))$, where the floating-point X is represented by an n -bit sequence. Correspondingly, the dequantization is $\bar{X} = X^q / (2^n - 1)$ at the decoder. In backpropagation, the quantization process is treated as an identity map. The architecture of the CNN-based SC framework is shown in Fig. 3.

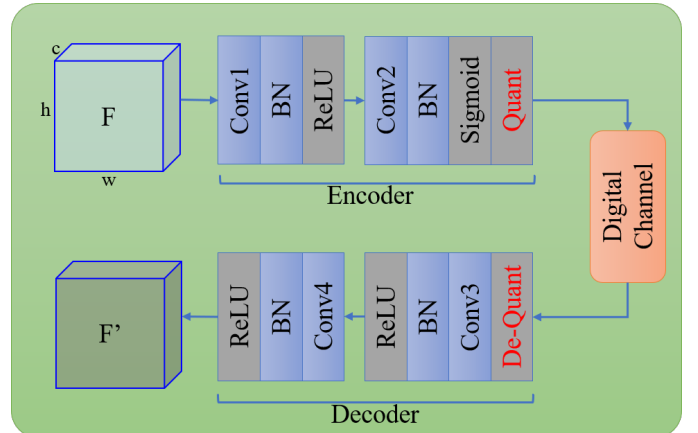


Fig. 3. The architecture of the CNN-based SC framework.

2) *Separate source and channel coding*: To perform the source and channel coding separately, we use the Joint photographic experts group (JPEG) for source coding and the convolutional code [65] for channel coding. Features are first quantized into 8-bit integers, then compressed by JPEG, and finally channel-coded by convolutional codes. The encoding result is input into the digital channel, and the receiver performs corresponding channel decoding, source decoding, and dequantization operations after receiving it.

C. Training Details

In this section, both the SNN-SC model and the baseline methods are used to extract semantic information of the feature from classification models in CI, and transmit them over digital channels. The split points we choose are the output of the 14th bottleneck block in ResNet50 with feature dimensions

TABLE I
THE PARAMETER SETTING OF THE SNN-SC

Module	Layer	Parameters
Encoder	Conv1	kernel size = 3, output = C/8
	Conv2	kernel size = 3, output = C/64
Reconstructor	Conv3	kernel size = 3, output = C/8
	Conv4	kernel size = 3, output = C
Converter	FCNN	input = $2n$, output = 1

(2048, 4, 4), and the output of the 10th convolutional layer in VGG16 with feature dimensions (512, 2, 2). We use convolutional layers to compress the feature's channels with $64\times$ compression ratio. For features with C channels, the parameter settings of the encoder, reconstructor, and converter in the SNN-SC model are shown in the Table I. The CNN-based baseline method uses the same settings in its encoder and decoder.

In the first step, the trained ResNet50 and VGG16 in our experiments are the same as those used in [20], achieving 77.81% and 74.04% accuracy on the CIFAR-100, respectively. In the second step, we train the SNN-SC model for 50 epochs with a batch size of 32, a learning rate of 10^{-4} and decayed by 2 every 10 epochs. In the third step, we train the whole model for 50 epochs with a batch size of 32, a learning rate of 10^{-5} and decayed by 2 every 10 epochs. The loss function used in second and third steps is Eq. (10), and α is set as 1.0. The firing thresholds of the IF and IHF are both set to 1, and the reset methods are soft reset. The training details of the CNN-based baseline method are the same, except for the loss function of the second and third steps. Since the binarization process of traditional quantization is non-differentiable, we cannot regularize the information entropy of the binarized bitstream, so we use the CE function in all training steps to train this baseline method.

Furthermore, in the second and third steps, the noisy digital channel is introduced to interfere with the semantic information bits according to a certain probability, and we fix the noise power during training (i.e., the bit error rate or bit erasure rate is fixed). In backpropagation, the noise interference of digital channel is treated as an identity map.

D. Model Performance

To ensure fairness, under the premise of transmitting the same number of bits on the channel, we compared the classification accuracy and robustness when using two different SC models to transmit classification model features. For example, if the CNN-based baseline method uses n -bit quantization, then the SNN-SC method will run n time steps to transmit the same number of bits. In the following simulations, n is set to 4 and 8. We train the SC models with different

classification models, under BSC and BEC with different bit error/erasure rates and transmission overheads, and then test their performance under different channel conditions in Fig. 4 and Fig. 5. The separate source and channel coding can be directly applied to the trained classification model. Furthermore, during performance evaluation, we repeat the semantic communication process 10 times to mitigate the effect of randomness introduced by the digital channel.

In the figures, SC_{SNN} , SC_{CNN} , and JPEG+Conv denote the performance of the classification model combined with the proposed SNN-SC model, the CNN-based baseline model, and the separate coding baseline model, respectively. The solid and dashed curves with the same color indicate the performance of the SC_{SNN} and SC_{CNN} , which are trained under the same channel conditions. The black dotted curves represent the performance of JPEG+Conv.

1) *Model Performance on ResNet50*: We study the performance of SNN-SC on ResNet50 in Fig. 4. Under BSC, we trained models under different bit error rates (i.e., $P_s = 0.15$ and 0.25) and different bandwidths (i.e., $n = 4$ and 8). Then we test the accuracy of these models on a range of bit error rates in Fig. 4(a) and Fig. 4(b). For SC_{SNN} and SC_{CNN} trained under the same bit error rate, we can observe that when the bit error rate is 0, that is, when there is no noise interference in the transmission process, the classification accuracy of SC_{SNN} and SC_{CNN} are both slightly lower than original ResNet50. This is because some information is lost during the compression and decompression process of the feature, but the performance loss caused by this is acceptable. As the channel bit error rate increases, the performance of both SC_{SNN} and SC_{CNN} will degrade due to noise interference. When the bit error rate is lower than 0.1, that is, when the channel condition is good, the performances of SC_{SNN} and SC_{CNN} are very close, and the performance drops very little. However, when the channel bit error rate is larger than 0.1, that is, when the channel condition is poor, we find that the performance of SC_{CNN} drops sharply, while that of SC_{SNN} gradually decreases. This phenomenon proves that SC_{SNN} is more robust than SC_{CNN} when disturbed by digital channel noise. There are two reasons why SC_{SNN} outperforms SC_{CNN} when digital channel conditions are poor. One is that the weights of bits in the conventional quantization result of SC_{CNN} are different. Bit errors with high weights introduce large errors, leading to large performance losses for SC_{CNN} , which occur more frequently with poorer channel conditions. However, SNN-SC uses spiking neurons to convert floating-point numbers into spikes, and the spikes are treated equally, so SNN-SC does not have this problem. Another reason is that the SNN neurons only fire when the membrane potential exceeds the threshold, which also helps the decoder filter out some membrane potential errors caused by channel interference.

For SC_{SNN} trained under different bit error rates, we find that the SC_{SNN} trained at $P_s = 0.25$ has a higher performance than the SC_{SNN} trained at $P_s = 0.15$ in poor channel conditions but exhibits slightly lower performance in good channel conditions. This behavior indicates that the SC_{SNN} determines an implicit trade-off between the robustness and performance. This can also be observed in SC_{CNN} .

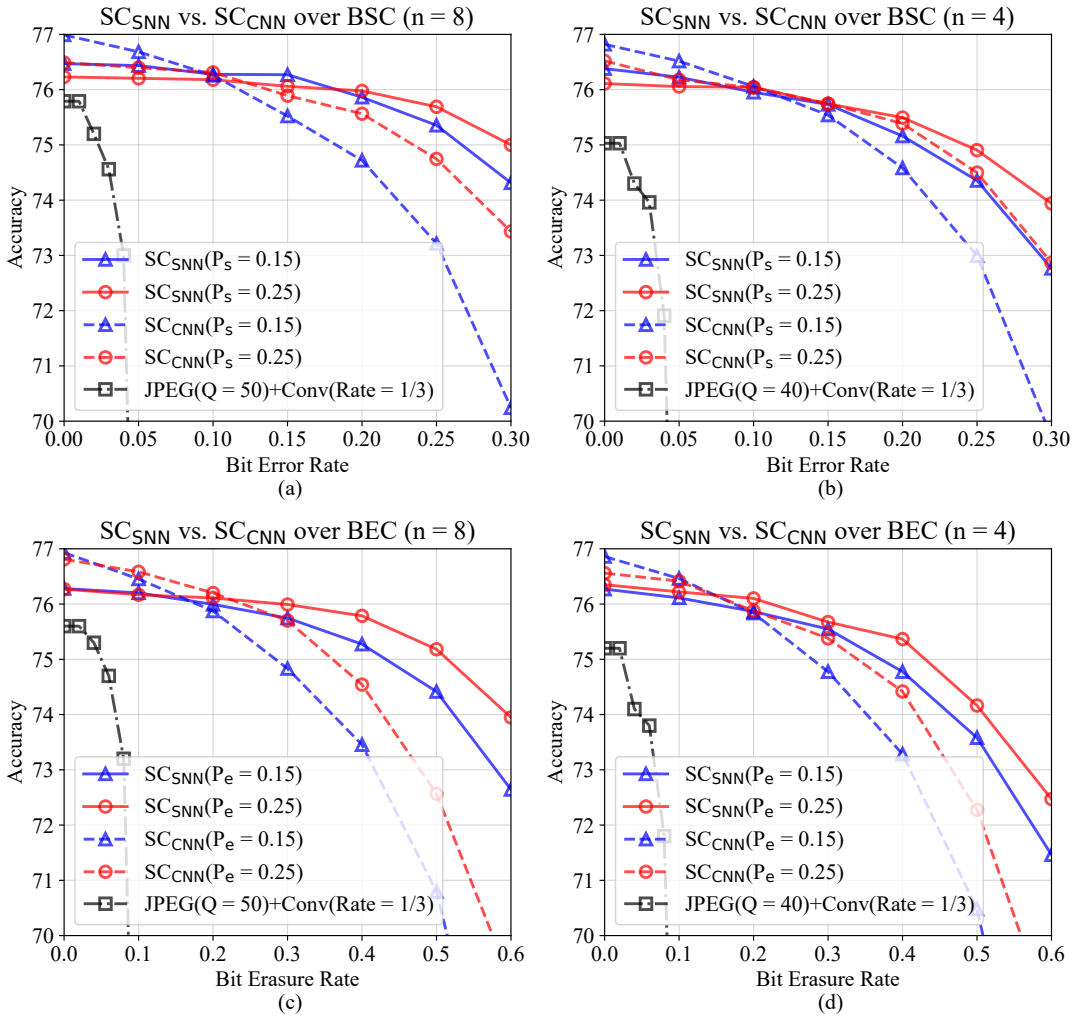


Fig. 4. Performance comparison between ResNet50 with SNN-SC and baseline over digital channels.

To achieve comparable performance to SC_{SNN} and SC_{CNN}, we use JPEG with a quality value of 50 (i.e., $Q = 50$) and convolutional code with a code rate of 1/3 (i.e., $\text{Rate}=1/3$) in JPEG+Conv. We can find that both SC_{SNN} and SC_{CNN} outperform JPEG+Conv, and they don't suffer from the 'cliff effect' in JPEG+Conv when the bit error rate is greater than 0.05. In addition, JPEG+Conv can only achieve about $5\times$ compression of features, which is much smaller than the $64\times$ compression of SC_{SNN} and SC_{CNN} for features.

The behavior of SC_{SNN}, SC_{CNN}, and JPEG+Conv are similar in $n = 8$ and $n = 4$ scenarios. While looking at the magnitude of change in accuracy, we can also see that the $n = 4$ model is less robust to noise than the $n = 8$ model due to the reduced amount of data transmitted.

On the other hand, we train SC_{SNN} and SC_{CNN} on BEC with bit erasure rates (i.e., $P_e = 0.15$ and 0.25) and different bandwidths (i.e., $n = 4$ and 8) in Fig. 4(c) and Fig. 4(d). The channel properties of BEC are different from those of BSC, the erased bit is randomly set to 0 or 1 before decoding at the receiver. Therefore, only half of the bits that are erased will be flipped. In this case, when the erasure rate of BEC is the

same as the bit error rate of BSC, BEC has less impact on the bit sequence than BSC. In the figures, SC_{SNN} and SC_{CNN} are tested on a wider range of bit erasure rates (i.e., 0-0.6), and the performance degrades significantly only when the bit erasure rate is greater than 0.3. Anyway, we can get a similar conclusion that SC_{SNN} has close classification accuracy to SC_{CNN} at low bit erasure rates, while SC_{SNN} has much better performance than SC_{CNN} at high bit erasure rates, and the performance of both is better than the traditional separate coding method JPEG+Conv.

2) *Model Performance on VGG16*: We study the performance of SNN-SC on VGG16 in Fig. 5. We train SC_{SNN} and SC_{CNN} under the same condition as before. For SC_{SNN} and SC_{CNN} trained under the same condition, when the channel condition is good, SC_{SNN} has very close classification accuracy to SC_{CNN}, and has much better performance when the channel condition is poor, whether it is BSC or BEC. The robustness of SC_{SNN} and SC_{CNN} will drop when n decreases. Moreover, the performance of JPEG+Conv is worse than SC_{SNN} and SC_{CNN}, and suffer from the 'cliff effect'. The compression ratio of JPEG+Conv is about $3\times$ which is

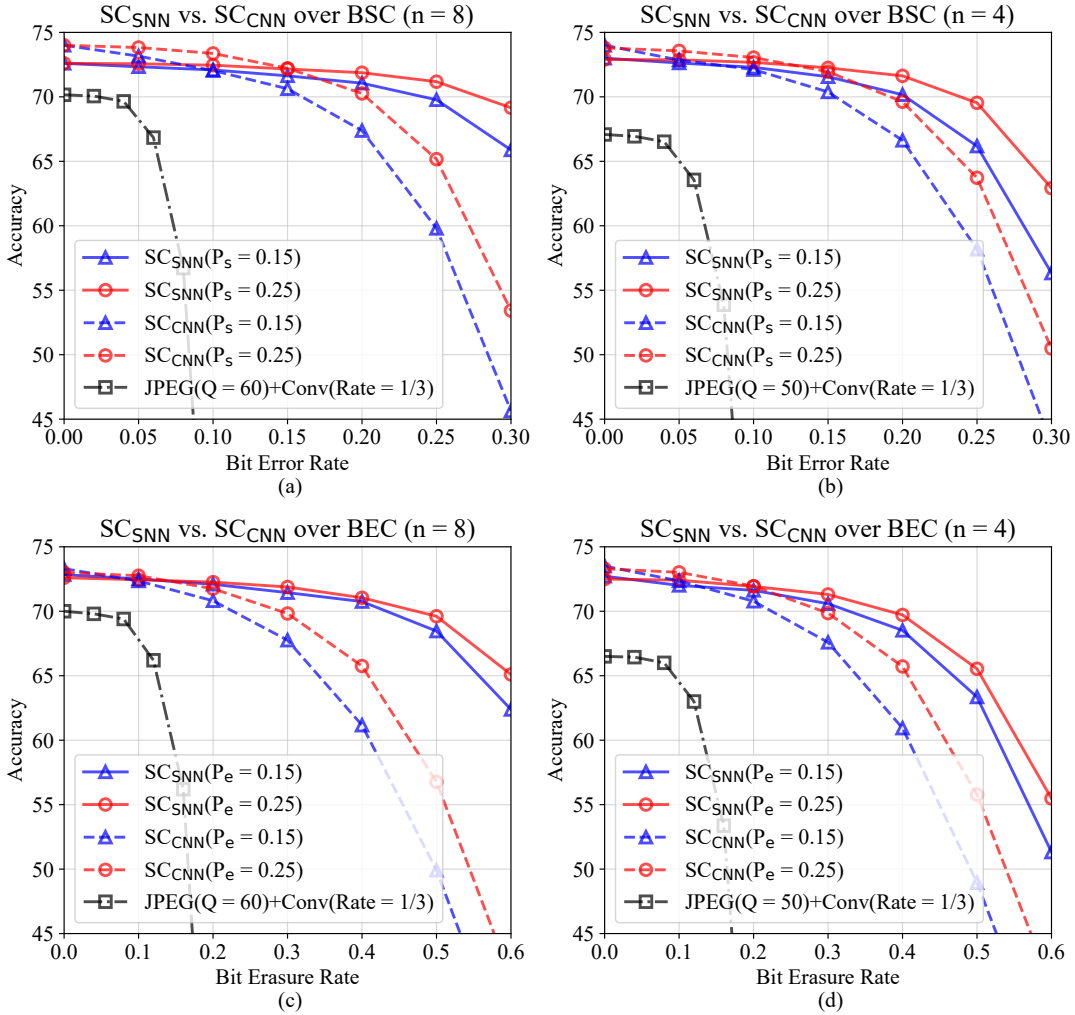


Fig. 5. Performance comparison between VGG16 with SNN-SC and baseline over digital channels.

much smaller than that of SC_{SNN} and SC_{CNN}. The behavior of SC_{SNN}, SC_{CNN}, and JPEG+Conv in Fig. 5 are similar to those in Fig. 4, which demonstrates the generalization ability of SNN-SC on different models. By comparing Fig. 5 and Fig. 4, we also find that the performance of VGG16 drops more sharply than ResNet50 as the bit error rate/erasure rate increases, because the simple structure of the VGG16 model makes the model more sensitive to noise.

In summary, these experiments show that our proposed SNN-SC model generalizes across different bandwidths, different channels, and different models. We can conclude that the proposed SNN-SC framework is more suitable than CNN-based SC model and separate source and channel coding model for feature SC on digital channels.

E. Ablation Studies

In this section, we aim to analyze the impact of the proposed IHF neuron and entropy-based regularization method on model performance. In order to ensure the persuasiveness of the experimental results, we adopt the method of controlling variables when conducting ablation experiments. In this section,

the classification model is ResNet50 and the digital channel we choose is BSC. In addition, except for the modules to be analyzed, other parts such as the training strategy, parameter settings of the spiking neurons, etc. are the same.

First, we design experiments to explore whether the two outputs of the IHF neurons both help SNN-SC to transmit semantic information. From the Eq. (8) we see that, if the membrane potential output is removed, the IHF will degenerate into an IF neuron. On the other hand, we will refer to an IHF neuron whose spike output is removed and only outputs membrane potential as an IHF-m neuron. Based on that, we refer to the SNN-SC framework with IHF, IF, and IHF-m neurons at the end of the reconstructor as the IHF model, IF model, and IHF-m model, respectively. We train these models using the CE function to remove the effect of entropy-based regularization on the models, and then evaluate the performance and robustness of these three models by performing feature SC on ResNet50.

We combine ResNet50 with the three models and train the combined models on the BSC with bit error rates of 0.15 and 0.25 (i.e., $P_s = 0.15$ and 0.25), respectively, and the test

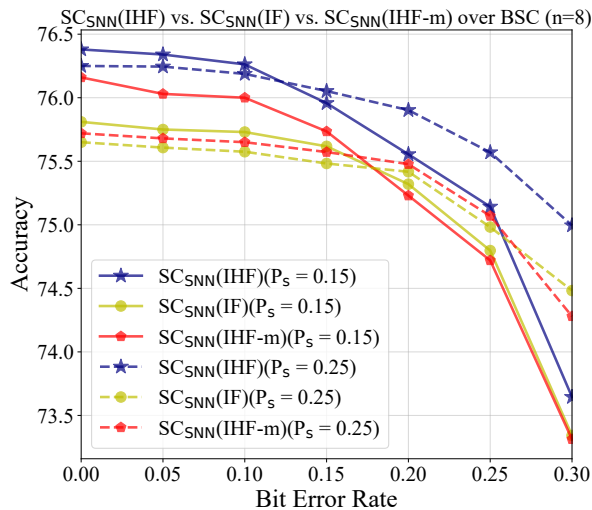


Fig. 6. Performance comparison between IHF model, IF model, and IHF-m model over BSC.

performance is shown in Fig. 6. In the figure, $SC_{SNN}(IHF)$, $SC_{SNN}(IF)$, and $SC_{SNN}(IHF-m)$ represent the test performance of ResNet50 with the IHF model, IF model, and IHF-m model, respectively. The solid lines indicate the test performance of the models trained on the BSC with the bit error rate of 0.15. Correspondingly, the dashed lines indicate the test performance of the models trained on the BSC with the bit error rate of 0.25. It is obvious that in the test bit error rate range, the performance of $SC_{SNN}(IHF)$ is much better than both $SC_{SNN}(IF)$ and $SC_{SNN}(IHF-m)$, regardless of training channel conditions. The reason is that the output of IHF contains more information than IF and IHF-m. IHF makes full use of the internal membrane potential information and external spike information of neurons, and enriches the input of the converter, making the reconstructed features more conducive to subsequent classification task inference.

From these experiments, we can conclude that IHF neurons have a more positive effect on feature SC compared to IF and IHF-m, and that both membrane potential and spiking contribute to the transmission performance of SNN-SC.

Secondly, we analyze the effect of regularizing the entropy of the extracted semantic information (i.e., the output of the encoder) during model training. Since IHF has been shown to have a positive effect on the model, we continued the ablation experiments based on the IHF model in the following part of this section.

To explore the impact of entropy of the extracted semantic information on model performance, we train IHF models with different α values in the regularization term. The training digital channel we choose is BSC with a bit error rate of 0.15, and then the trained IHF models are tested over a range of bit error rates. According to Eq. (10), calculating the information entropy of semantic information H requires the probability of 0 and 1 (i.e., p_0 and p_1), and $p_0 + p_1 = 1$. We obtain the frequencies of 0 and 1 in the semantic information through statistics and then use them as approximate estimates of p_0 and p_1 respectively. The IHF model with regularization is called

the IHF+Reg model. The test results of the ResNet50 with different IHF+Reg models are shown in Fig. 7.

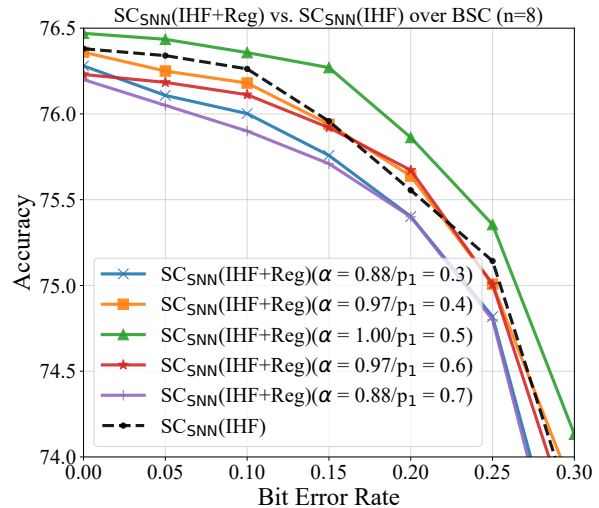


Fig. 7. Performance of the models with different regularization terms.

In Fig. 7, $SC_{SNN}(IHF+Reg)$ represents the ResNet50 with IHF+Reg model. The dotted line is the test performance of the IHF model without regularization, and the solid lines are the IHF+Reg models with different α values. We find that as the value of α increases, the performance of the model also increases. When α is 1.0, the performance and robustness of the model are the best, and correspondingly, the entropy of the extracted semantic information is limited to a maximum value of 1.0 (i.e., $p_0 = p_1 = 0.5$).

In information theory [66], the entropy of a random variable is the average level of “information”. When the entropy is 1.0, it means that the amount of information contained in the semantic information reaches the maximum. In this case, the semantic information contains the most information related to cloud classification tasks, so the performance of the model is the best.

In summary, entropy can measure the amount of task-related information contained in the extracted semantic information, and maximizing the entropy of semantic information through regularization terms will have a positive impact on model performance.

V. CONCLUSION

In this paper, we propose a SNN-based semantic communication framework, SNN-SC, for the transmission of features in CI over digital channels. By jointly designing the semantic encoder and the semantic decoder for extracting the essential semantic information, the proposed SNN-SC can handle the task-related semantic information effectively. Since the outputs of SNN neuron are binary spikes, the SNN-SC framework can be directly applied to digital channels without an explicit quantization.

Furthermore, we propose a novel spiking neuron called IHF and a entropy-based regularization term to improve the performance and robustness of the model. Both IHF and the

regularization term have been verified to have a positive impact on the model.

Moreover, the proposed SNN-SC framework is combined with classification models in CI to verify its effectiveness, which is the first attempt to bridge the gap between SNN and digital semantic communication. Finally, the SNN-SC framework is trained and tested on different classification models, digital channels and bandwidths, and the experimental results all show that it outperforms the CNN-based semantic communication framework under poor channel conditions, and overcomes the ‘cliff effect’ in the traditional separate coding method. This work also points out a new direction for the follow-up study of semantic communication.

REFERENCES

- [1] H. Choi and I. V. Bajić, “Deep feature compression for collaborative object detection,” in *2018 25th IEEE International Conference on Image Processing (ICIP)*. IEEE, 2018, pp. 3743–3747.
- [2] H. Choi and I. V. Bajić, “Near-lossless deep feature compression for collaborative intelligence,” in *2018 IEEE 20th International Workshop on Multimedia Signal Processing (MMSP)*. IEEE, 2018, pp. 1–6.
- [3] S. Ma, X. Zhang, S. Wang, X. Zhang, C. Jia, and S. Wang, “Joint feature and texture coding: Toward smart video representation via front-end intelligence,” *IEEE Transactions on Circuits and Systems for Video Technology*, vol. 29, no. 10, pp. 3095–3105, 2018.
- [4] S. R. Alvar and I. V. Bajić, “Multi-task learning with compressible features for collaborative intelligence,” in *2019 IEEE International Conference on Image Processing (ICIP)*. IEEE, 2019, pp. 1705–1709.
- [5] S. Suzuki, S. Takeda, M. Takagi, R. Tanida, H. Kimata, and H. Shouno, “Deep feature compression using spatio-temporal arrangement toward collaborative intelligent world,” *IEEE Transactions on Circuits and Systems for Video Technology*, 2021.
- [6] C. E. Shannon, “A mathematical theory of communication,” *The Bell system technical journal*, vol. 27, no. 3, pp. 379–423, 1948.
- [7] J. Bao, P. Basu, M. Dean, C. Partridge, A. Swami, W. Leland, and J. A. Hendler, “Towards a theory of semantic communication,” in *2011 IEEE Network Science Workshop*. IEEE, 2011, pp. 110–117.
- [8] Y. LeCun, Y. Bengio, and G. Hinton, “Deep learning,” *nature*, vol. 521, no. 7553, pp. 436–444, 2015.
- [9] T. O’shea and J. Hoydis, “An introduction to deep learning for the physical layer,” *IEEE Transactions on Cognitive Communications and Networking*, vol. 3, no. 4, pp. 563–575, 2017.
- [10] H. Ye, G. Y. Li, and B.-H. Juang, “Deep learning based end-to-end wireless communication systems without pilots,” *IEEE Transactions on Cognitive Communications and Networking*, vol. 7, no. 3, pp. 702–714, 2021.
- [11] P. Jiang, C.-K. Wen, S. Jin, and G. Y. Li, “Deep source-channel coding for sentence semantic transmission with harq,” *IEEE Transactions on Communications*, 2022.
- [12] X. Luo, H.-H. Chen, and Q. Guo, “Semantic communications: Overview, open issues, and future research directions,” *IEEE Wireless Communications*, 2022.
- [13] H. Xie, Z. Qin, G. Y. Li, and B.-H. Juang, “Deep learning enabled semantic communication systems,” *IEEE Transactions on Signal Processing*, vol. 69, pp. 2663–2675, 2021.
- [14] H. Xie and Z. Qin, “A lite distributed semantic communication system for internet of things,” *IEEE Journal on Selected Areas in Communications*, vol. 39, no. 1, pp. 142–153, 2020.
- [15] E. Boursoulatte, D. B. Kurka, and D. Gündüz, “Deep joint source-channel coding for wireless image transmission,” *IEEE Transactions on Cognitive Communications and Networking*, vol. 5, no. 3, pp. 567–579, 2019.
- [16] M. Ding, J. Li, M. Ma, and X. Fan, “Snr-adaptive deep joint source-channel coding for wireless image transmission,” in *ICASSP 2021-2021 IEEE International Conference on Acoustics, Speech and Signal Processing (ICASSP)*. IEEE, 2021, pp. 1555–1559.
- [17] J. Xu, B. Ai, W. Chen, A. Yang, P. Sun, and M. Rodrigues, “Wireless image transmission using deep source channel coding with attention modules,” *IEEE Transactions on Circuits and Systems for Video Technology*, vol. 32, no. 4, pp. 2315–2328, 2021.
- [18] S. Wang, K. Yang, J. Dai, and K. Niu, “Distributed image transmission using deep joint source-channel coding,” in *ICASSP 2022-2022 IEEE International Conference on Acoustics, Speech and Signal Processing (ICASSP)*. IEEE, 2022, pp. 5208–5212.
- [19] M. Jankowski, D. Gündüz, and K. Mikołajczyk, “Deep joint source-channel coding for wireless image retrieval,” in *ICASSP 2020-2020 IEEE International Conference on Acoustics, Speech and Signal Processing (ICASSP)*. IEEE, 2020, pp. 5070–5074.
- [20] J. Shao and J. Zhang, “Bottlenet++: An end-to-end approach for feature compression in device-edge co-inference systems,” in *2020 IEEE International Conference on Communications Workshops (ICC Workshops)*. IEEE, 2020, pp. 1–6.
- [21] M. Wang, Z. Zhang, J. Li, M. Ma, and X. Fan, “Deep joint source-channel coding for multi-task network,” *IEEE Signal Processing Letters*, vol. 28, pp. 1973–1977, 2021.
- [22] P. Wang, J. Li, M. Ma, and X. Fan, “Distributed audio-visual parsing based on multimodal transformer and deep joint source channel coding,” in *ICASSP 2022-2022 IEEE International Conference on Acoustics, Speech and Signal Processing (ICASSP)*. IEEE, 2022, pp. 4623–4627.
- [23] Y. Kang, J. Hauswald, C. Gao, A. Rovinski, T. Mudge, J. Mars, and L. Tang, “Neurosurgeon: Collaborative intelligence between the cloud and mobile edge,” *ACM SIGARCH Computer Architecture News*, vol. 45, no. 1, pp. 615–629, 2017.
- [24] F. Zhai, Y. Eisenberg, and A. K. Katsaggelos, “Joint source-channel coding for video communications,” *Handbook of Image and Video Processing*, pp. 1065–1082, 2005.
- [25] M. Jankowski, D. Gündüz, and K. Mikołajczyk, “Joint device-edge inference over wireless links with pruning,” in *2020 IEEE 21st International Workshop on Signal Processing Advances in Wireless Communications (SPAWC)*. IEEE, 2020, pp. 1–5.
- [26] J. Shao, Y. Mao, and J. Zhang, “Learning task-oriented communication for edge inference: An information bottleneck approach,” *IEEE Journal on Selected Areas in Communications*, vol. 40, no. 1, pp. 197–211, 2021.
- [27] J. Shao, H. Zhang, Y. Mao, and J. Zhang, “Branchy-gnn: A device-edge co-inference framework for efficient point cloud processing,” in *ICASSP 2021-2021 IEEE International Conference on Acoustics, Speech and Signal Processing (ICASSP)*. IEEE, 2021, pp. 8488–8492.
- [28] Y. Zhang, W. Xu, H. Gao, and F. Wang, “Multi-user semantic communications for cooperative object identification,” in *2022 IEEE International Conference on Communications Workshops (ICC Workshops)*. IEEE, 2022, pp. 157–162.
- [29] W. Maass, “Networks of spiking neurons: the third generation of neural network models,” *Neural networks*, vol. 10, no. 9, pp. 1659–1671, 1997.
- [30] W. Fang, Z. Yu, Y. Chen, T. Masquelier, T. Huang, and Y. Tian, “Incorporating learnable membrane time constant to enhance learning of spiking neural networks,” in *Proceedings of the IEEE/CVF International Conference on Computer Vision*, 2021, pp. 2661–2671.
- [31] A. Tavanaei, M. Ghodrati, S. R. Kheradpisheh, T. Masquelier, and A. Maida, “Deep learning in spiking neural networks,” *Neural networks*, vol. 111, pp. 47–63, 2019.
- [32] C. Xu, Y. Liu, D. Chen, and Y. Yang, “Direct training via backpropagation for ultra-low-latency spiking neural networks with multi-threshold,” *Symmetry*, vol. 14, no. 9, p. 1933, 2022.
- [33] J. Kim, H. Kim, S. Huh, J. Lee, and K. Choi, “Deep neural networks with weighted spikes,” *Neurocomputing*, vol. 311, pp. 373–386, 2018.
- [34] Y. Chen, Y. Mai, R. Feng, and J. Xiao, “An adaptive threshold mechanism for accurate and efficient deep spiking convolutional neural networks,” *Neurocomputing*, vol. 469, pp. 189–197, 2022.
- [35] K. Patel, E. Hunsberger, S. Batir, and C. Eliasmith, “A spiking neural network for image segmentation,” *arXiv preprint arXiv:2106.08921*, 2021.
- [36] S. Kim, S. Park, B. Na, and S. Yoon, “Spiking-yolo: spiking neural network for energy-efficient object detection,” in *Proceedings of the AAAI conference on artificial intelligence*, vol. 34, no. 07, 2020, pp. 11 270–11 277.
- [37] Y. Cao, Y. Chen, and D. Khosla, “Spiking deep convolutional neural networks for energy-efficient object recognition,” *International Journal of Computer Vision*, vol. 113, no. 1, pp. 54–66, 2015.
- [38] W. Fang, Z. Yu, Y. Chen, T. Huang, T. Masquelier, and Y. Tian, “Deep residual learning in spiking neural networks,” *Advances in Neural Information Processing Systems*, vol. 34, pp. 21 056–21 069, 2021.
- [39] X. Xiang, L. Zhu, J. Li, Y. Wang, T. Huang, and Y. Tian, “Learning super-resolution reconstruction for high temporal resolution spike stream,” *IEEE Transactions on Circuits and Systems for Video Technology*, 2021.

- [40] J. Devlin, M.-W. Chang, K. Lee, and K. Toutanova, "Bert: Pre-training of deep bidirectional transformers for language understanding," *arXiv preprint arXiv:1810.04805*, 2018.
- [41] Q. Zhou, R. Li, Z. Zhao, Y. Xiao, and H. Zhang, "Adaptive bit rate control in semantic communication with incremental knowledge-based harq," *IEEE Open Journal of the Communications Society*, vol. 3, pp. 1076–1089, 2022.
- [42] Y. Zhang, H. Zhao, J. Wei, J. Zhang, M. F. Flanagan, and J. Xiong, "Context-based semantic communication via dynamic programming," *IEEE Transactions on Cognitive Communications and Networking*, vol. 8, no. 3, pp. 1453–1467, 2022.
- [43] S. Yao, K. Niu, S. Wang, and J. Dai, "Semantic coding for text transmission: An iterative design," *IEEE Transactions on Cognitive Communications and Networking*, vol. 8, no. 4, pp. 1594–1603, 2022.
- [44] Y. Wang, H. Yao, and S. Zhao, "Auto-encoder based dimensionality reduction," *Neurocomputing*, vol. 184, pp. 232–242, 2016.
- [45] W. F. Lo, N. Mital, H. Wu, and D. Gündüz, "Collaborative semantic communication for edge inference," *IEEE Wireless Communications Letters*, 2023.
- [46] S. Lu and A. Sengupta, "Exploring the connection between binary and spiking neural networks," *Frontiers in Neuroscience*, vol. 14, p. 535, 2020.
- [47] E. Ledinauskas, J. Ruseckas, A. Juršėnas, and G. Buračas, "Training deep spiking neural networks," *arXiv preprint arXiv:2006.04436*, 2020.
- [48] B. Han, G. Srinivasan, and K. Roy, "Rmp-snn: Residual membrane potential neuron for enabling deeper high-accuracy and low-latency spiking neural network," in *Proceedings of the IEEE/CVF conference on computer vision and pattern recognition*, 2020, pp. 13 558–13 567.
- [49] L. Zhu, X. Wang, Y. Chang, J. Li, T. Huang, and Y. Tian, "Event-based video reconstruction via potential-assisted spiking neural network," in *Proceedings of the IEEE/CVF Conference on Computer Vision and Pattern Recognition*, 2022, pp. 3594–3604.
- [50] H. Jang, N. Skatchkovsky, and O. Simeone, "Spiking neural networks—part i: Detecting spatial patterns," *IEEE Communications Letters*, vol. 25, no. 6, pp. 1736–1740, 2021.
- [51] B. Rueckauer, I.-A. Lungu, Y. Hu, M. Pfeiffer, and S.-C. Liu, "Conversion of continuous-valued deep networks to efficient event-driven networks for image classification," *Frontiers in neuroscience*, vol. 11, p. 682, 2017.
- [52] W. Fang, Z. Yu, Y. Chen, T. Huang, T. Masquelier, and Y. Tian, "Deep residual learning in spiking neural networks," *Advances in Neural Information Processing Systems*, vol. 34, pp. 21 056–21 069, 2021.
- [53] E. O. Neftci, H. Mostafa, and F. Zenke, "Surrogate gradient learning in spiking neural networks: Bringing the power of gradient-based optimization to spiking neural networks," *IEEE Signal Processing Magazine*, vol. 36, no. 6, pp. 51–63, 2019.
- [54] Y. Wu, L. Deng, G. Li, J. Zhu, Y. Xie, and L. Shi, "Direct training for spiking neural networks: Faster, larger, better," in *Proceedings of the AAAI Conference on Artificial Intelligence*, vol. 33, no. 01, 2019, pp. 1311–1318.
- [55] S.-i. Ikegawa, R. Saiin, Y. Sawada, and N. Natori, "Rethinking the role of normalization and residual blocks for spiking neural networks," *Sensors*, vol. 22, no. 8, p. 2876, 2022.
- [56] N. Skatchkovsky, H. Jang, and O. Simeone, "End-to-end learning of neuromorphic wireless systems for low-power edge artificial intelligence," in *2020 54th Asilomar Conference on Signals, Systems, and Computers*. IEEE, 2020, pp. 166–173.
- [57] A. Cassidy, Z. Zhang, and A. G. Andreou, "Impulse radio address event interconnects for body area networks and neural prostheses," in *2008 Argentine School of Micro-Nanoelectronics, Technology and Applications*. IEEE, 2008, pp. 87–92.
- [58] J. Chen, N. Skatchkovsky, and O. Simeone, "Neuromorphic wireless cognition: event-driven semantic communications for remote inference," *IEEE Transactions on Cognitive Communications and Networking*, 2023.
- [59] N. Rathi and K. Roy, "Diet-snn: A low-latency spiking neural network with direct input encoding and leakage and threshold optimization," *IEEE Transactions on Neural Networks and Learning Systems*, 2021.
- [60] K. He, X. Zhang, S. Ren, and J. Sun, "Deep residual learning for image recognition," in *Proceedings of the IEEE conference on computer vision and pattern recognition*, 2016, pp. 770–778.
- [61] A. Krizhevsky, G. Hinton *et al.*, "Learning multiple layers of features from tiny images," 2009.
- [62] K. Simonyan and A. Zisserman, "Very deep convolutional networks for large-scale image recognition," in *International Conference on Learning Representations*, May 2015.
- [63] A. Paszke, S. Gross, F. Massa, A. Lerer, J. Bradbury, G. Chanan, T. Killeen, Z. Lin, N. Gimelshein, L. Antiga *et al.*, "Pytorch: An imperative style, high-performance deep learning library," *Advances in neural information processing systems*, vol. 32, 2019.
- [64] W. Fang, Y. Chen, J. Ding, D. Chen, Z. Yu, H. Zhou, Y. Tian, and other contributors, "Spikingjelly," <https://github.com/fangwei123456/spikingjelly>, 2020, accessed: 2021-07-03 (0.0.0.0.6).
- [65] P. Elias, "Coding for noisy channels," in *IRE International Convention Record*, 1955, pp. 37–46.
- [66] S. Kullback, *Information theory and statistics*. Courier Corporation, 1997.